https://doi.org/10.31436/iiumej.v26i1.3221

WEARABLE TEXTILE PATCH DSSRS ANTENNA FOR BODY TUMORS DETECTION WITH REDUCED SAR

M.M. HASAN MAHFUZ[1], MD RAFIQUL ISLAM[2*], NORUN FARIHAH ABDUL MALEK[2], MOHAMED HADI HABAEBI[2], NAZMUS SAKIB[3], ELHAM BALADI[4]

[1]*Department of Electrical and Computer Engineering, Concordia University, Montreal, QC, Canada*
[2]*Department of Electrical and Computer Engineering, International Islamic University Malaysia*
[3]*Graduate School of Science and Technology, Gunma University, Japan*
[4]*Department of Electrical Engineering, Polytechnique Montréal, QC, Canada*

**Corresponding author: rafiq@iium.edu.my*

(Received: 12 March 2024; Accepted: 6 September 2024; Published online: 10 January 2025)

ABSTRACT: The purpose of this study is to present a lightweight wearable (jeans) monopole antenna configuration for body area network (BAN) communication, breast and head tumors detections with back lobe reduction (i.e., low SAR), and it does so without introducing any special methodologies like as, AMC, EBG, HIS. The planned antenna has dual symmetrical slots as well as a ring-shaped slot (DSSRS) at the top, and it is in the form of a radiating rectangular patch with a ground plane. The design procedure has been finished with the help of CST MWS, and the next step will be to fine-tune the parameters of the antenna structure to achieve resonance at the ISM band (5.79 GHz). Testing for BAN, breast, and brain tumor detection was done using this prototype. With the proper impedance matching, the antenna achieves an operational bandwidth of 5.798 GHz (5.739–5.865 GHz), 5.77 GHz (5.715–5.838 GHz), 5.77 GHz (5.718–5.843 GHz) and 5.78 GHz (5.725–5.834 GHz), with an overall peak gain of 8.18 dBi, 7.69 dBi, 5.73 dBi, and 4.59 dBi; when proposed antenna placed on the free space, on the body, on the breast, and the head respectively. The suggested antenna meets the specific absorption rate (SAR) standards given by the FCC (1 gm) and the ICNIRP (10 gm).

ABSTRAK: Kajian ini bertujuan untuk membentangkan konfigurasi antena monopole ringan boleh pakai (jenis jeans) untuk komunikasi rangkaian kawasan badan (BAN), pengesanan tumor payudara dan kepala dengan pengurangan lobus belakang (iaitu, SAR rendah), tanpa menggunakan metodologi khas seperti AMC, EBG, atau HIS. Antena yang dicadangkan mempunyai dua slot simetri (dual symmetrical slots) serta slot berbentuk cincin (DSSRS) di bahagian atas, dan berbentuk patch segi empat tepat yang memancar dengan satah tanah. Prosedur reka bentuk telah diselesaikan dengan bantuan perisian CST MWS, dan langkah seterusnya adalah untuk menyesuaikan parameter struktur antena bagi mencapai resonans pada jalur ISM (5.79 GHz). Ujian untuk BAN, pengesanan tumor payudara, dan tumor otak telah dijalankan menggunakan prototaip ini. Dengan padanan impedans yang betul, antena ini mencapai lebar jalur operasi sebanyak 5.798 GHz (5.739–5.865 GHz), 5.77 GHz (5.715–5.838 GHz), 5.77 GHz (5.718–5.843 GHz), dan 5.78 GHz (5.725–5.834 GHz), dengan pencapaian keuntungan puncak keseluruhan sebanyak 8.18 dBi, 7.69 dBi, 5.73 dBi, dan 4.59 dBi; apabila antena yang dicadangkan diletakkan di ruang bebas, pada badan, pada payudara, dan pada kepala masing-masing. Antena yang dicadangkan memenuhi piawaian kadar penyerapan spesifik (SAR) yang ditetapkan oleh FCC (1 gm) dan ICNIRP (10 gm).

KEYWORDS: Antenna, Microwave, Wideband, Cancer, Breast phantom, Tumor detection

https://doi.org/10.31436/iiumej.v26i1.3221

1. INTRODUCTION

In order to collect data about the user's personal health or, more broadly, to interface with the user, wearable technology includes gadgets that consumers can easily wear and use for lengthy periods of time inconspicuously, such as clothing or accessories [1]. At present, smart accessories like smartwatches, wristbands, smart glasses, and other garments clip-on account for the vast majority of the market share held by wearable devices [2]. Wearable gadgets like these often incorporate preexisting small sensors and electronics into compact packages [3]. As a result of their inflexible and nonflexible construction, they are not well suited to the creation of increasingly sophisticated wearable devices, which call for increased skin-to-device contact and an enhanced user interface. Micro and nano-electronics integrated into textile substrates are useful in creating smart materials with improved ergonomics or "smart textiles" [4]. Smart textile technology has the potential to enable the development of a broad range of capabilities on a textile substrate, previously only possible in rigid and nonflexible electronic goods [3], [5]. Many people became curious about electronic textiles because of this promising prospect [6], [7]. Rapid advances in technology, small gadgets, and mobile computing are fueling a market for wearable technologies that are predicted to continue growing at a compound annual growth rate of 15.5%. Recent market forecasts predict that the wearable devices industry will grow to more than USD 155 billion by 2027, in large part due to the participation of many large companies that are increasing their research efforts to switch from uncomfortable wearable electronics hardware to more comfortable smart textile [8].

Manufacturers are being encouraged by the rising consumer demand to create and commercialize billions of wearable electronics devices in a variety of market segments, such as health and wellness, military and defense, space exploration, fashion, and entertainment [9], [10]. Healthcare is one of the most promising markets, propelled by customers' growing desire to continuously monitor their health or be monitored by healthcare professionals who need to have more health data available to them so they may more thoroughly analyze a wider cohort of patients [11]. Smart biomedical clothing's comfort and accessibility could be crucial components of ongoing, long-term clinical monitoring. These cutting-edge devices can be integrated into Internet of Things (IoT) networks, utilizing straightforward but effective wireless solutions to create smart systems for remote health monitoring, allowing patients to continue living at home instead of spending money on expensive healthcare facilities. Having continuous, noninvasive, and seamless surveillance of health and physical well-being allows people to live independently and actively in their own houses, which is one of the key functions of wearable health monitoring devices [12]. This is a huge benefit, especially for people dealing with long-term medical conditions or having trouble moving around. The use of wearable monitoring systems highlights two additional benefits for users: first, it lessens the influence and stress that the clinical environment exerts on patient performance, and second, the massive amount of data gathered with this system can be processed by AI algorithms to detect a possible worsening of a patient's clinical situation [13]Smart wearable biomedical systems have the potential to offer advanced services to patients from the perspective of the public health system by combining frequently worn material with the most technologically advanced sensing, processing, and communicating capabilities. They can also support health cost reduction through the facilitation of early hospital discharges.

The essential criteria for comfortable wearing materials are compact size, flexibility, resilience, low SAR, and low power requirements [14], [15]. The SAR measures how much energy is transmitted through human tissue. The absorption of electromagnetic energy could potentially be harmful to human health. So, it's crucial to consider SAR when designing wearable antennas. The SAR must be significantly lower than the minimum allowed level. To

https://doi.org/10.31436/iiumej.v26i1.3221

safeguard the public from excessive exposure to EM fields, many organizations, such as the IEEE, ICNIRP, and the FCC, have proposed limitations on the radiation released by these devices. The FCC and ICNIRP require a SAR of less than 2 W/kg averaged over 10 gm and less than 1.6 W/kg averaged over 1 gm of human tissue [1], [16-17]. However, the battery life of ISM (Industrial, Scientific, and Medical) equipment is increased, and it does not require a lot of energy to send a signal to the receiver. Fabrics intended for use as clothing are a particularly promising option for developing flexible antennas. This is because fabric antennas can be readily sewn into the fabric. A highly effective, highly gain-flexible antenna can be conceived and fabricated by fusing ISM (2.4 & 5.8 GHz) and textile technologies. For BAN applications, the bending performance of the wearable textile antenna is typically a significant consideration. However, the bending effects are less significant for tumor detection in areas such as the breast or head. This is because the garments used in these applications, such as a female bra or a head cap, are more stable and consistent in shape compared to regular clothing worn on other parts of the body [18], [19]. The stretchy antenna might be concealed within the fabric of jeans. This approach has been followed in microwave scattered technology for tumor detection. When the tumors are present inside the human body (breast, head) model, the S_{11} response of the antenna system is successfully altered.

1.1. Specific Absorption Rate (SAR)

SAR measures the rate at which energy is absorbed by the human body when exposed to a radio frequency (RF) electromagnetic field. It's commonly used to quantify the exposure levels from devices. SAR is expressed in watts per kilogram (W/kg) and indicates how much RF energy is absorbed per unit mass of tissue. There are some key points for SAR:

- **Measurement:** SAR values are determined through laboratory testing using standardized procedures. These tests simulate the human body's exposure to RF energy.
- **Regulatory Limits:** In the United States, the Federal Communications Commission (FCC) limits SAR to 1.6 W/kg, averaging over 1 gm of tissue. In Europe, the limit is 2.0 W/kg, averaging over 10 gm of tissue, as per the International Commission on Non-Ionizing Radiation Protection (ICNIRP) guidelines.
- **Health and Safety:** Regulatory agencies set SAR limits to ensure that exposure stays within safe levels, minimizing potential health risks. Ongoing research investigates the long-term effects of RF exposure to ensure that the guidelines remain current with scientific findings. SAR can be calculated using the following formula:

$$SAR = \frac{\sigma E^2}{\rho} \quad (1)$$

where σ is the electrical conductivity of the tissue (measured in Siemens per meter, S/m), E is the root mean square (RMS) electric field strength (measured in volts per meter, V/m), and ρ is the mass density of the tissue (measured in kilograms per cubic meter, kg/m³).

1.2. Motivation

Recent research has focused on using S_{11} for tumor detection, whereas AMC and UWB antennas have been used for skin cancer detection [20]. The scattering parameter (S_{11}) was used in this paper to evaluate the difference between cancerous and normal skin tissues. Those research works in [19-23] have focused on antenna design for breast and skin cancer detection. The work in [26] has also focused on the use of S_{11} for the detection of cancer cells. It uses a flexible antenna design and microwave scattering parameters for tumor detection. Brain tumor detection using an antenna was also studied in [27] and [28], utilizing changes in the S_{11}

https://doi.org/10.31436/iiumej.v26i1.3221

parameter as an indicator. The references in these above-cited works also present previous studies on the use of changes in S_{11} as an indicator for several types of cancer. The work in this field is still in progress and has neither been finalized nor clinically approved or adopted for detection, but it is a research area. Combining the S_{11} changes with other techniques may help in more accurate diagnosis and detection procedures. Hence, the work in this manuscript is motivated.

1.3. Novelty and Contribution

A new patch configuration comprising a circular slot with two parallel adjacent rectangular slots was designed, and its performance details were evaluated using simulation models. The contribution of this work is as follows:

- A motivation for using a flexible patch antenna for jeans fabrication and the change in S_{11} to detect the presence of breast cancer is presented.
- A novel patch design comprising a circular slot with two parallel rectangular slots resonating at the ISM band is presented.
- A sweep parametric study was conducted to achieve optimal results at resonance.
- The parameters like S_{11}, VSWR, gain, and radiation pattern were evaluated and presented.

The following is the research article's structure. The first part of this article provided a high-level overview of potential uses for wearable antennas. In Section 2, the various types of recent wearable antennas, together with their performance characteristics and prospective applications, are presented to the reader. Section 3 illustrated the DSSRS antenna's design, simulated results, and bending effect on different radii. Section 4 shows the DSSRS antenna's performance on the different parts of the human body, such as the body, breast, and head. This section also discussed the SAR values during breast and head tumor detection. Finally, section 5 shows the conclusion part of this research article.

2. RECENT RELATED WORKS

Recently published articles related to the suggested work are mentioned here. Wearable applications of coplanar keyhole antenna, including the design of novel antenna on fabric substrates for interfacing with internal and external sensors, are described [29]. The process of designing the fabrication method of screen printing on fabric substrates is explained using conductive inks available for purchase on the market. Antenna resonance at 5.8 GHz is discussed, as well as the impacts of wash durability and the inks' resistance to deterioration over time when used as interface layers between conductive elements and fabric substrates of coplanar keyhole fabric antenna. This research [30] introduces a compact AMC wearable textile antenna optimized for 5.8 GHz band Wireless Body Area Network (WBAN) applications in the ISM band. For these reasons, better antenna performance and shielding from harmful back radiation Artificial Magnetic Conductor (AMC) structure was implemented. The antenna with the built-in AMC has a measured gain of 8.92 dBi, efficiency of 80%, impedance bandwidth of 1.4 GHz (24.1%), and SAR values of 0.00103 W/Kg for 10 gm and 0.00034 W/Kg for 1 gm tissues. Wearable on-body scenarios using the suggested antenna were investigated with a multi-layer computational model of the human body. Each human tissue layer's thickness and its potential impact were studied. Antenna performance was maintained, consistent gain was achieved, and SAR values were below IEEE recommendations for wearer safety.

https://doi.org/10.31436/iiumej.v26i1.3221

To boost the antenna's impedance bandwidth, this study proposes a rectangular eight-shaped Electromagnetic Band Gap (EBG) structure operating in the 5.8 GHz ISM band for wearable applications [31]. Ansys HFSS High-Frequency Structure Simulator's Eigenmode solution simulates the eight-shaped EBG unit cell. An inverted E-shape monopole antenna operating at 5.8 GHz is also used to show the successful use of the proposed EBG. As a result of the band stop property of EBG construction, surface waves are reduced, and a wearable antenna's back lobe also experiences a reduction. The Internet of Things (IoT) gives a boost to the latest generation of wearable devices. Textile antennas are developed, and they can be completely integrated into garments. An on-body single patch and multiple-input multiple-output (MIMO) textile (Taffeta fabric) antenna was presented in this study [32]. The findings confirmed the constructed antenna's viability at the specified frequency (5.8 GHz). Frequency shifts and other performance issues, such as those caused by the pressure used during the eyelet attachment procedure, are possible consequences of making textile antennas by hand. For use in medical telemetry, the suggested antenna [33] has been optimized for design and construction. A rising area of study, biocompatible antenna design is essential in pollution-controlled environments for telemetry systems used in patient monitoring, elderly health monitoring, children's safety, and firefighter's safety. Denim is offered as the substrate for a unique E-shaped textile antenna to be used in patient telemetry. Biocompatibility, miniaturization, and operation in the ISM band at 2.45 GHz.

On the other hand, by simulating a common scenario for WBAN applications, this research [34] measures the influence of mechanical curvature on a textile inset-fed microstrip patch antenna placed above a human head phantom. Therefore, this study evaluates how operational properties, including resonance frequency, bandwidth, and radiation pattern, are affected by body proximity and antenna curvature. In addition, the SAR of the cranium was determined and compared to global safeguarding requirements. Computational studies reveal that when the antenna is applied to a human head, the curvature of the antenna produces a significant change in the resonant frequency. Therefore, the antenna's bandwidth must be sufficiently high in the first place to compensate for this negative effect. The developed antenna achieved a front-to-back ratio of 19 dB to reduce brain radiation exposure. This research [35] suggested using an AMC-backed leather antenna that operates in the ISM 5.8 GHz band. Leather substrate allows the antenna and AMC to be worn with casual attire. The suggested antenna has good impedance matching within the ISM band at 5.8 GHz, and its reflection coefficient was unaffected by crumpling and bending. The suggested antenna has a 90% reduction in SAR value compared to the antenna alone, making it acceptable for use by the general public. The design's return loss and SAR performance also degrades very little when the human body is loaded. The proposed AMC-supported wearable antenna is a viable option for use in the medical field. As a wearable antenna for use in the ISM band at a central frequency of 2.45 GHz, this study [36] introduces an antenna based on the Mercedes-Benz insignia, with a metal plate placed at an optimized distance from the suggested antenna. To optimize the radiation performance of the suggested design, decrease the back radiation, and lower the SAR when loaded on a human body, a metal plate is integrated with the antenna to serve as an isolator and reflector. The suggested antenna, coplanar waveguide-fed, was printed on a Rogers 4003C substrate and has dimensions of 35 mm × 35 mm × 0.508 mm. Its impedance bandwidth is (2.20–2.56) GHz, and its gain was 7.3 dB at 2.45 GHz. The SAR was lower than the criteria the FCC and the ICNIRP set.

An easily transportable asymmetric coplanar strip-fed comb-shaped patch (CSP) antenna made of textile was presented [37] and investigated for use in the Medical Body Area Network and the ISM band. Denim has been implanted with a thin piece of highly conductive fabric to create a flexible, conductive, wearable antenna. The CSP antenna has been tested in open areas

and worn. The proposed CSP antenna has a free space resonance frequency of 2.49 GHz (2.27–3.42) GHz and an operating frequency range of 1150 MHz. When worn on the body, the antenna has a 900 MHz bandwidth and 2.44 GHz (1.9–2.8) GHz resonance frequency. In open space, the gain is measured at 4.67 dBi, which drops to –4.82 dBi when used on a human body. The CSP antenna has been crumpled and bent without affecting its performance. For use in the ISM band, a unique, miniature implantable antenna has been proposed [38]. The suggested antenna was a circular patch antenna with a shape; it was designed using information from existing studies, and its smaller size was accomplished using various downsizing methods. The radiating structure was patched with a circular shape and features square fillet edges. The ground plane was extended to cover the entire plane, eliminating the back reflections. This antenna structure operates at 2.45 GHz with the preferred omnidirectional pattern to maximize compatibility with other in-body devices. Within the ISM band, modeling, designing, and fabrication of a wearable pentagon microstrip patch antenna were carried out [39]. Its medical uses include diagnosing diseases like brain cancer and examining images of the head. In order to choose, simulate, and carry out the design most effectively, it is necessary to compute the patch's physical dimensions, including the matching circuits. The simulation tool utilizes a human head model to calculate SAR. This study will provide preliminary results that can be used for future development of technologies involving wearable antennas, and it will also make it easier to design additional innovative detecting methods.

3. DESIGN, SIMULATION, AND PARAMETRIC ANALYSIS OF DSSRS ANTENNA

Typically, microstrip patch antennas are the best option for wearable applications due to their flexibility and ease of incorporation [1]. The wearable antenna design must be simple and use flexible, versatile building materials. A variety of material characteristics affect an antenna's performance [40]. The rectangular patch antenna is often used due to its superior layout compared to other patch antennas [41]. Due to their compact size and adaptability, microstrip and patch antennas are widely used. Fabric construction means it is lightweight and compact design is ideal for human use [42]. The developed antenna has significant utility for investigating health-related parameters. The simulation processes are performed using the CST MWS. The antenna substrate is a piece of denim fabric (jeans). Jeans fabric is an attractive substrate for textile antennas due to its durability, stiffness, low density, and low cost [43]. On a jeans substrate, dual symmetrical slots and a ring-shaped slot (DSSRS) top on the radiating patch antenna were developed with a height of 1 mm, relative permittivity of 1.7, and loss tangent of 0.025. Copper material is used for the conducting patch and the ground plane, and each of these components has a thickness of 0.035 mm. Eqs. (2) to (9) were utilized to design initial circular slot rectangular slots. The optimized values of width (W_p = 45 mm), patch length (L_p = 46.1 mm), feedline width (W_f = 3.6 mm), and ring-shape slot diameter (R = 12 mm) are obtained through simulation. Figure 1 shows a representation of the simulated antenna.

$$W_p = \frac{c}{2f_r\sqrt{\frac{\varepsilon_r+1}{2}}} \tag{2}$$

$$\varepsilon_{eff} = \frac{\varepsilon_r+1}{2} + \frac{\varepsilon_r-1}{2}\left[1 + 12\frac{h}{W_p}\right]^{-\frac{1}{2}} \tag{3}$$

$$L_{eff} = \frac{c}{2f_r\sqrt{\varepsilon_{ff}}} \tag{4}$$

https://doi.org/10.31436/iiumej.v26i1.3221

$$\Delta L = 0.412h\frac{(\varepsilon_{eff}-0.3)\left(\frac{W_p}{h}+0.264\right)}{(\varepsilon_{eff}-0.258)\left(\frac{W_p}{h}+0.8\right)} \quad (5)$$

$$L_p = L_{eff} - 2\Delta L \quad (6)$$

$$W_f = \frac{7.48h}{e^{z_0\frac{\sqrt{\varepsilon_r+1.41}}{87}}} - 1.25t \quad (7)$$

$$R = F\left\{1+\frac{2h}{\pi\varepsilon_r F}\left[\ln\left(\frac{\pi F}{2h}\right)\right]+1.7726\right\}^{-\frac{1}{2}} \quad (8)$$

$$F = \frac{8.791\times10^9}{f_r\sqrt{\varepsilon_r}} \quad (9)$$

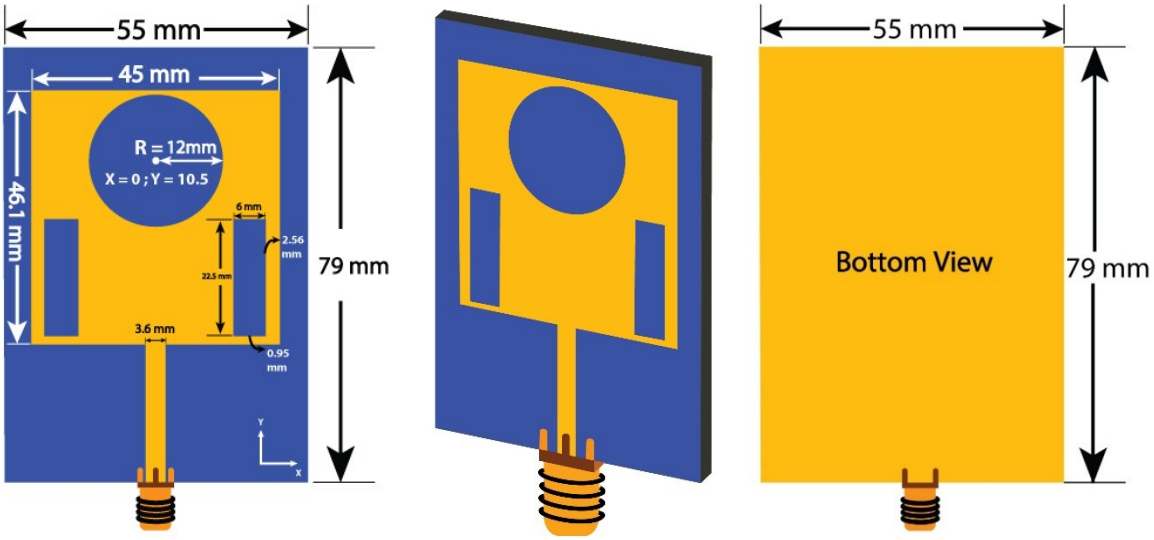

(a) Front View (b) Side View (c) Bottom View

Figure 1. The proposed DSSRS antenna

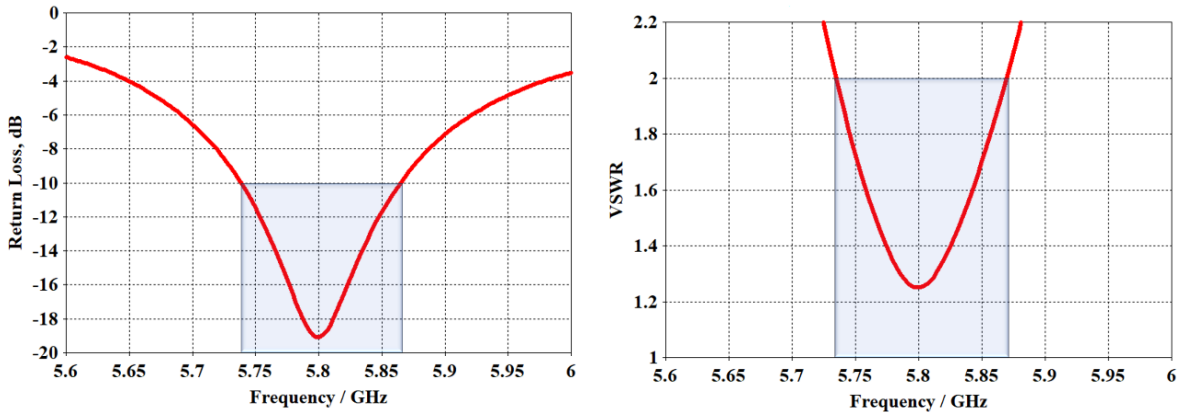

(a) (b)

Figure 2. The simulated (a) return loss & (b) VSWR of the DSSRS antenna

The return loss can refer to the reflection coefficient, which can be represented by the symbol S_{11}. Specifically, it is the ratio of incident power to reflected power. The reflection coefficient must be high (or at least satisfactory). An antenna needs S_{11} of at least –10 dB and preferably more than –15 dB [44]. As shown in Figure 2(a), the simulated antenna has a return

https://doi.org/10.31436/iiumej.v26i1.3221

loss of –19.068 dB at 5.798 GHz while maintaining a respectable level of bandwidth (5.739–5.865 GHz). Another name for it is the voltage standing wave ratio (written as VSWR). It is put to use in the process of determining matches. The magnitude of the mismatch increases proportionately with the VSWR value. The suggested antenna has a VSWR ratio of 1.251 at 5.798 GHz, as illustrated in Figure 2(b).

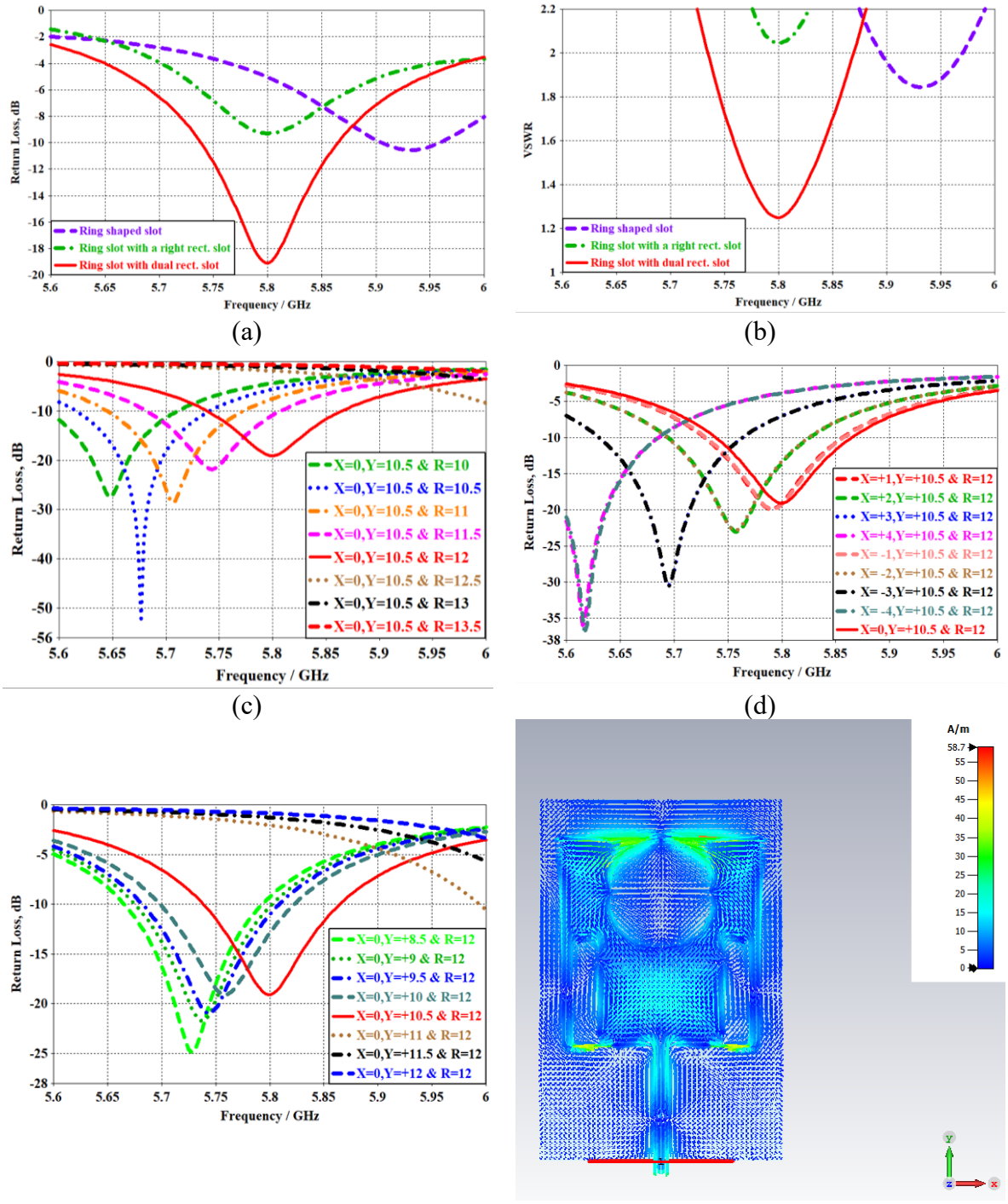

Figure 3. The parametric studies of (a, b) ring-shaped slots with dual symmetrical rectangular slots S_{11}, VSWR and S_{11} of (c) altering the radius of the ring-shaped slot, (d) altering the X-axis values, (e) altering the Y-axis values & (f) surface current (58.7 A/m) at 5.798 GHz

https://doi.org/10.31436/iiumej.v26i1.3221

Figures 3(a) and (b) show the S_{11} and VSWR of the ring-shaped slots with dual symmetrical rectangular slots parametric studies. This study clearly shows that the DSSRS proposed antenna operates at 5.79 GHz. Figure 3(c)(d)(e) is sufficient proof that X=0, Y=10.5 mm, and R=12 mm have an excellent performance of the proposed antenna. However, Figure 3(c) shows the S_{11} study while the X, Y-axis constant just altering R values. Figure 3(d)(e) illustrates the changing of X, Y-axis values. The remaining parameters (Y, X-axis, R) values are constant. The surface current accumulating of 58.7 A/m at 5.798 GHz, as shown in Figure 3(f), which supports that the DSSRS, the antenna resonates at 5.798 GHz and it exhibits high magnitude at the edges and maximum current distribution at the center of the patch at the resonant frequency. This distribution strongly depends on the height of the substrate, which is crucial for determining the antenna size. However, due to the DSSRS, the antenna resonates at a frequency f_r =5.798 GHz. From the surface current, as shown in Figure 3(f), it is clear that the DSSRS significantly impacts the entire bandwidth.

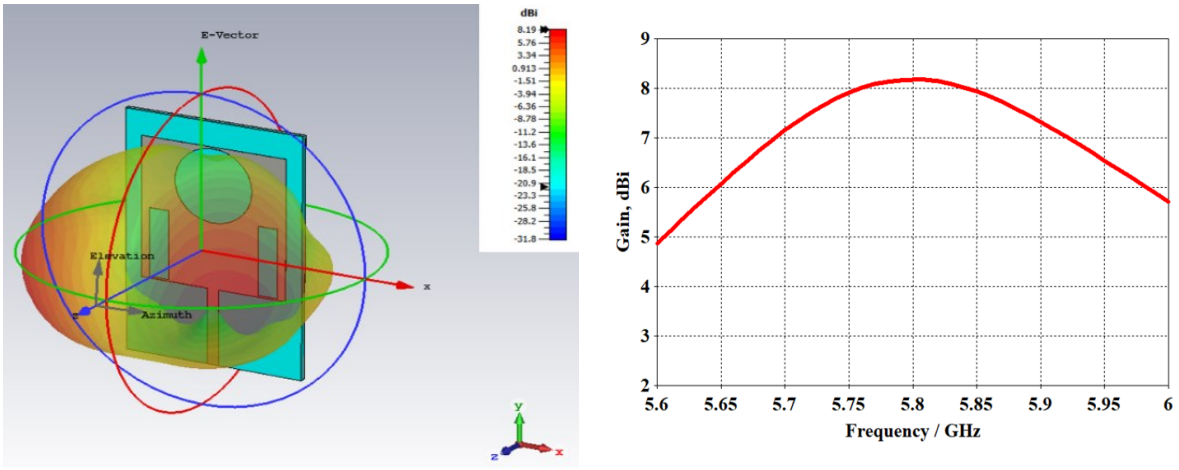

(a) (b)

Figure 4. The simulated (a) 3-D radiation pattern and (b) Gain

Figure 4(a)(b) shows the simulated 3D radiation pattern and gain (8.19 dBi at 5.798 GHz), respectively. An important performance metric is the antenna gain, calculated by adding the directivity to the antenna's radiation efficiency. The amount of input power an antenna can successfully convert into radio frequency that travels in a certain direction is called its gain. It has been determined that the proposed antenna has a gain of 8.18 dBi at resonant frequency = 5.798 GHz. To determine the radiated power level, it is necessary to observe the radiation pattern. For wearable antennas to be useful, they must be able to resist performance degradation when bent or stretched.

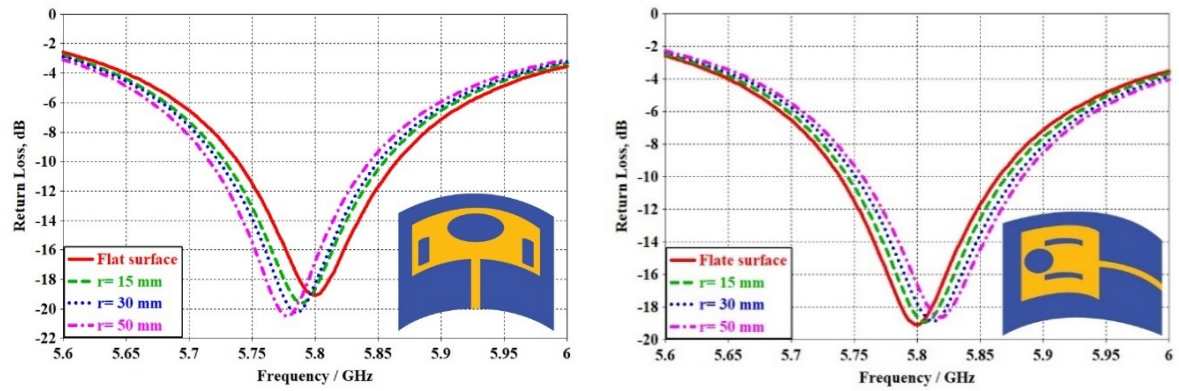

(a) E-plane (b) H-plane

https://doi.org/10.31436/iiumej.v26i1.3221

Figure 5. Comparisons of return loss for the antenna at varying bending radii

Figure 5 shows the simulated return loss of the proposed antenna in the E and H planes, respectively, for three alternative radii (15, 30 & 50 mm). The suggested antenna has improved impedance matching, as seen in Figure 5(a), with a return loss of less than –10 dB for all E-plane bending radii. With a return loss for the H-plane below –10 dB, Figure 5(b) illustrates that the suggested antenna exhibits a superior impedance-matching response. It is important to note that both the antenna's E and H-plane resonant frequencies are slightly delayed left and right (compared to the flat counterpart). Despite this, the fractional bandwidths of the bent antenna vary from 128 MHz to 130 MHz, which can be considered almost the same regardless of all bending (15, 30 & 50 mm) circumstances. The slot combination was chosen to exploit complementary effects on electromagnetic properties, resulting in a compact design suitable for various body configurations. It minimized the bending effects, as shown in Figure 5.

4. PERFORMANCE EVALUATION OF DSSRS ANTENNA FOR BODY APPLICATIONS

4.1. On Body

Since the human body has lossy properties, the antenna's performance changes as it gets closer to a person's body. A human phantom with four layers evaluates the antenna's performance. Figure 6 shows that the four layers of the human phantom are composed of dry skin, fat, muscles, and cortical bone, with corresponding thicknesses of 2 mm, 3.5 mm, and 10 mm [45]. As can be seen in Figure 6, the proposed antenna’s performance simulation on the human body.

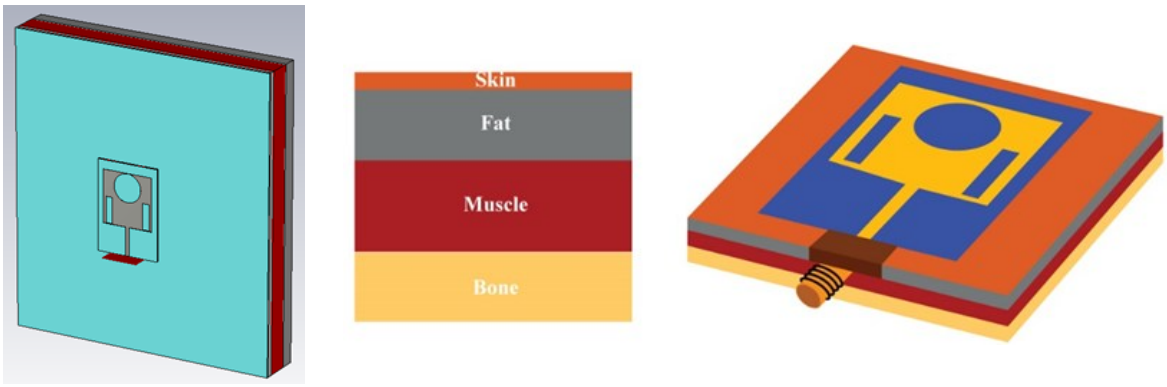

(a) (b)

Figure 6. Prototype (a, b) of the proposed antenna mounted on the human body

Figure 7(a)(b) displays the simulated return loss and VSWR obtained by fastening the antenna to a human body, and the resonant frequency lightly shifted from 5.798 GHz to 5.77 GHz. An excellent impedance match is achieved with minimal frequency shift when the antenna is placed on a human body, as seen by the fractional bandwidth of 2.146%. Figure 7(c) illustrates the 3-D radiation pattern performed at 5.77 GHz (5.715–5.838 GHz) on the human body. Because of the pattern's form, the antenna exhibits Z-plane directional radiation and a maximum gain of 7.69 dBi (Figure 7d), making it suitable for on-body communications. When the antenna was placed for realistic on-body applications, it was supposed to be incorporated into a suit, and then it would be subject to bending.

https://doi.org/10.31436/iiumej.v26i1.3221

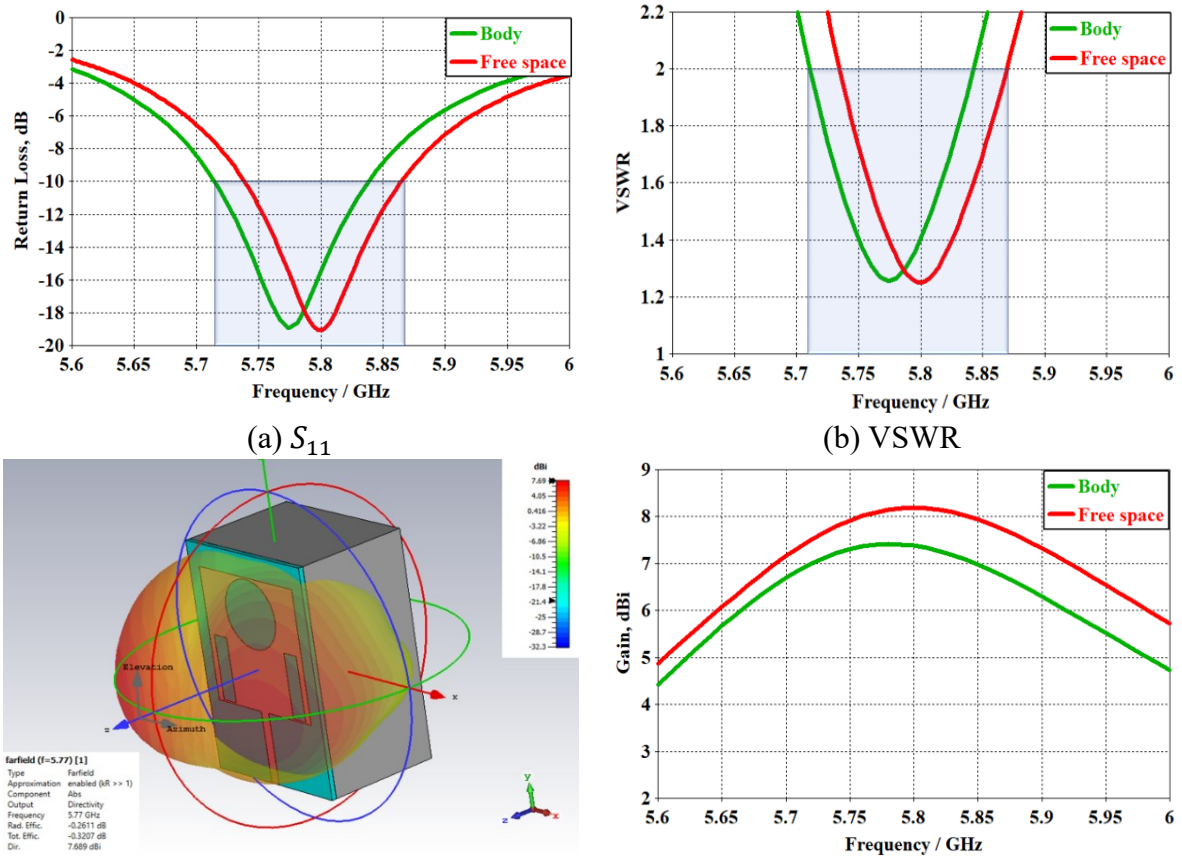

(a) S_{11} (b) VSWR

(c) 3D Radiation Pattern at 5.77 GHz (d) Gain

Figure 7. The simulated results of the DSSRS antenna

Thus, the consequences of bending on the human body have been studied for the E and H-plane in different radii (15, 30, 50 mm) and illustrated in Figure 8. As can be seen in Figure 8, when the antenna is bent, the detuning of the resonant frequency is accentuated. The fractional bandwidths of the bent antenna vary from 128 MHz to 130 MHz for all bending (15, 30 & 50 mm) circumstances, which are similar, as shown in Figure 5, without a body.

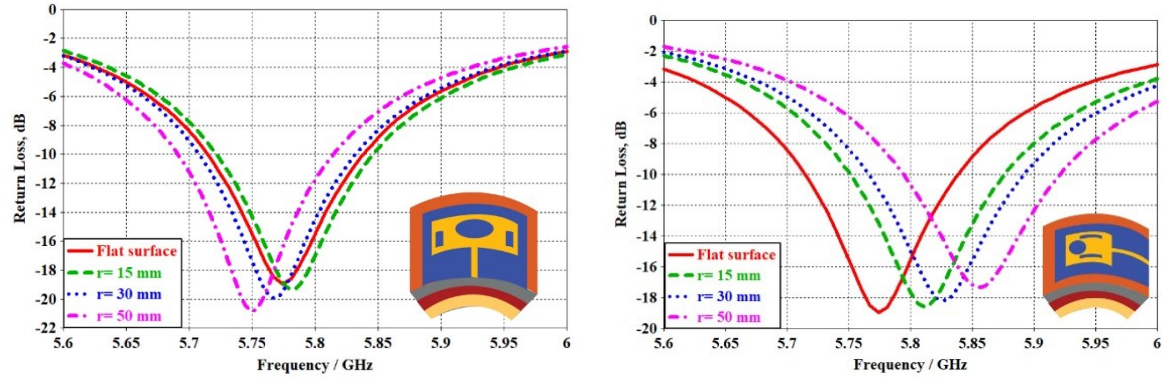

(a) E-plane (b) H-plane

Figure 8. Comparisons of S_{11} for the antenna on the body at varying bending radii

Figure 9 depicts a simulation of the SAR at 5.77 GHz, performed following the FCC (1 gm) and ICNIRP (10 gm) regulations. Maximum SAR values were 0.00000662 W/kg for 1 gm of tissue and 0.0000027 W/kg for 10 gm. As a result, the completed design was compatible

https://doi.org/10.31436/iiumej.v26i1.3221

with both the United States and the European Union's SAR criteria, and it can be suggested as a wearable antenna for ISM band applications.

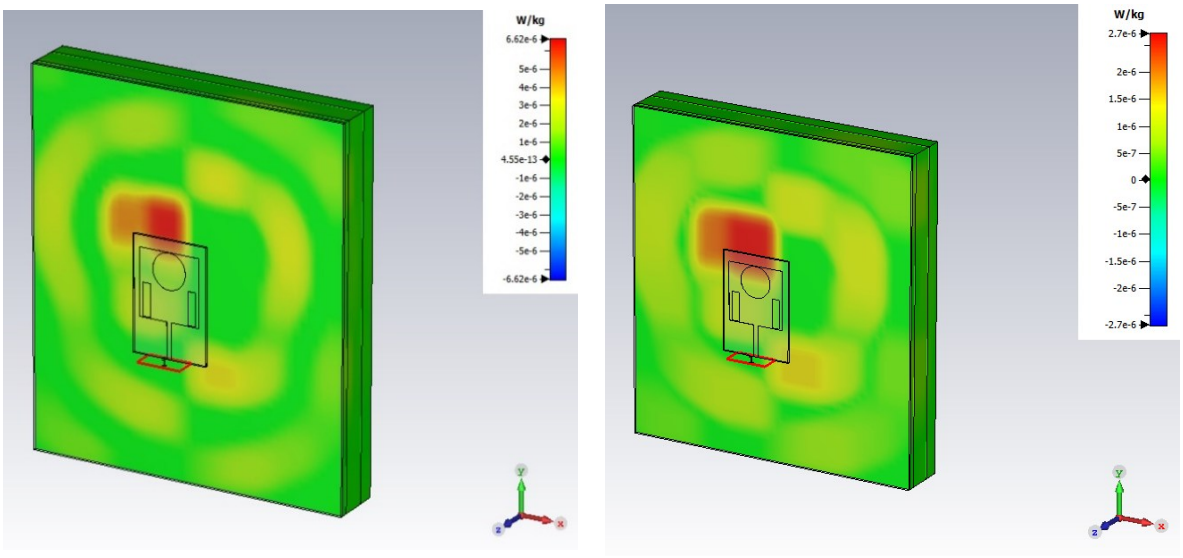

(a) 1 gm (0.00000662 W/kg) (b) 10 gm (0.0000027 W/kg) tissue

Figure 9. The SAR evaluation at 5.77 GHz

4.2. On Breast

Female breast cancer is increasingly common, making early detection crucial for prompt treatment. Conventional methods of tumor detection are both costly and time-consuming [46]. Because of the dispersed S_{11} values, it has been determined that tumors alter the relative permittivity and conductivity of the tissues in the vicinity of tumors. The identification of breast tumors was the primary objective of the antenna. Specific dielectric and thermal properties (ε_r=5.08, σ=0.13 [S/m], thermal conductivity, δ=0.33 [W/(m*K)], specific heat, θ=[2550J/(kg*K)], density, d=1041[kg/m^3] were associate with the breast phantom [47]. This study aimed to examine the relationship between return loss and the condition of a breast phantom. A simulation was run using CST MWS with the textile (jeans) antenna placed on the normal breast phantom, as illustrated in Figure 10.

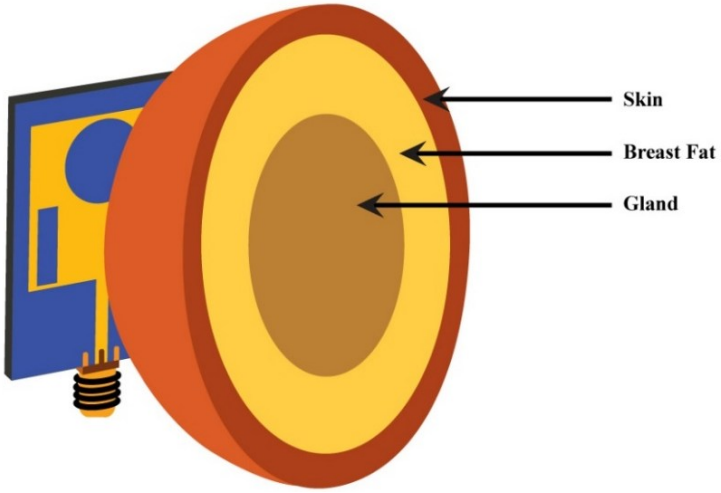

Figure 10. The 3-D model of a healthy breast phantom

https://doi.org/10.31436/iiumej.v26i1.3221

There was a –19.128 dB attenuation for a healthy breast's reflection coefficient at 5.77 GHz, as shown in Figure 11(a), and the VSWR in Figure 11(b). The VSWR<2 means the proposed antenna has excellent impedance matching on the breast phantom environment. Figure 11(c)(d) illustrates the 3-D radiation pattern and gain. Gain has been achieved at 5.73 dBi in breast phantom at 5.77 GHz, with a z-axis directional.

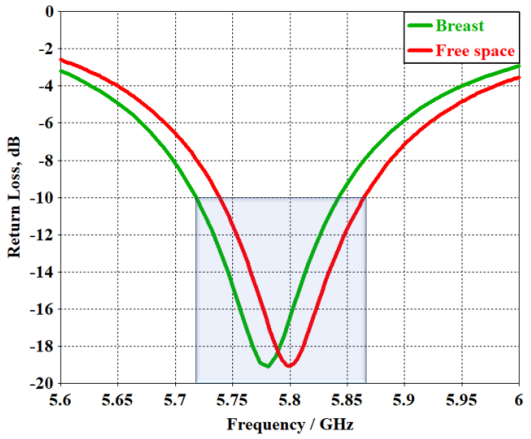

(a) S_{11}

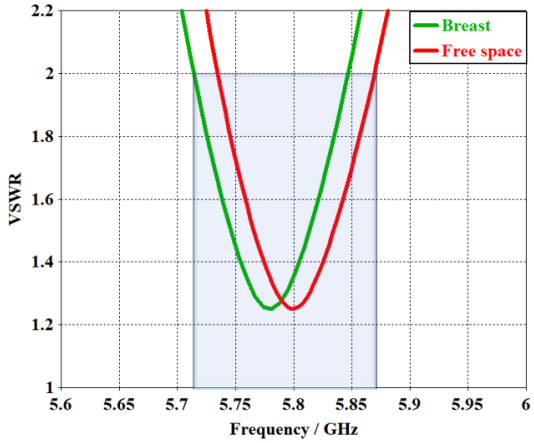

(b) VSWR

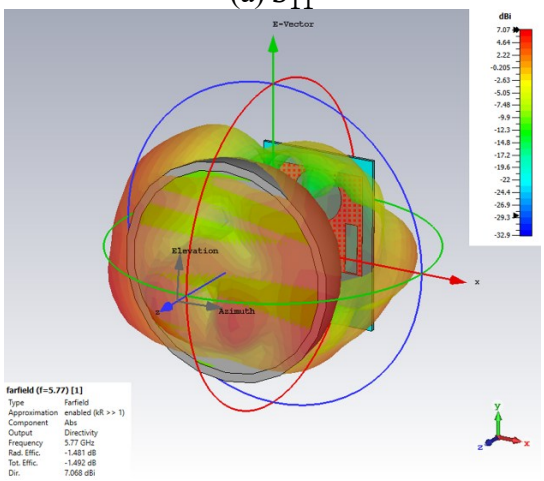

(c) 3D Radiation Pattern at 5.78 GHz

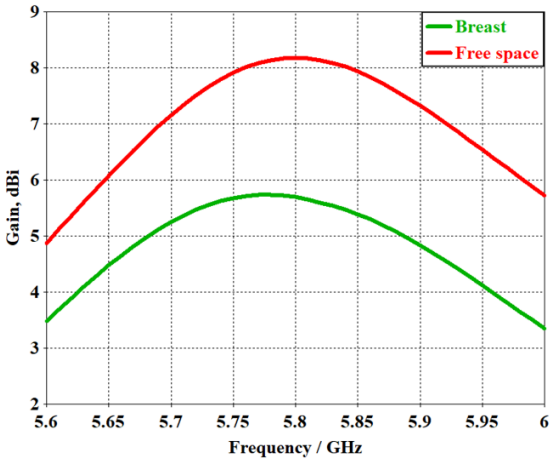

(d) Gain

Figure 11. The textile antenna was placed on a phantom of a healthy breast

The SAR value was 0.651 W/Kg for 1 gm of tissue and 0.419 W/Kg for 10 gm of tissue, as shown in Figure 12. This value was quite low compared to the necessary maximum level. The characteristics of fictitious tumors in the breast are shown in Figure 13(a) (ε_r=59.06, σ=3[S/m], δ=0.5[W/(m*K)]). The unhealthy breast tissue is augmented using those values. Figure 13(b) displays the simulated S_{11}, which is attenuated by –18.283 dB, –17.967 dB & –18.349 dB to 10, 20 and 30 mm radii tumor sizes. These simulations aim to test the antenna's performance in the presence of tumors in a breast phantom. The return loss value is slightly higher than in normal tissues, and the resonance frequencies are shifted towards the left as tumor sizes increase in breast tumors, as shown in Figure 13(b).

https://doi.org/10.31436/iiumej.v26i1.3221

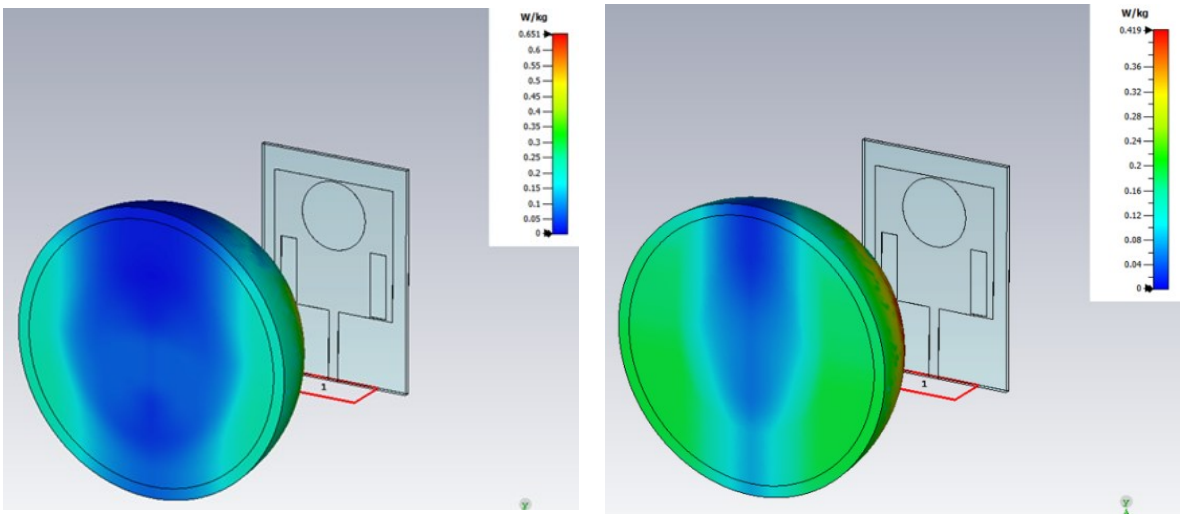

(a) 1 gm (0.651 W/Kg) (b) 10 gm (0.419 W/Kg) tissue

Figure 12. The simulated SAR value

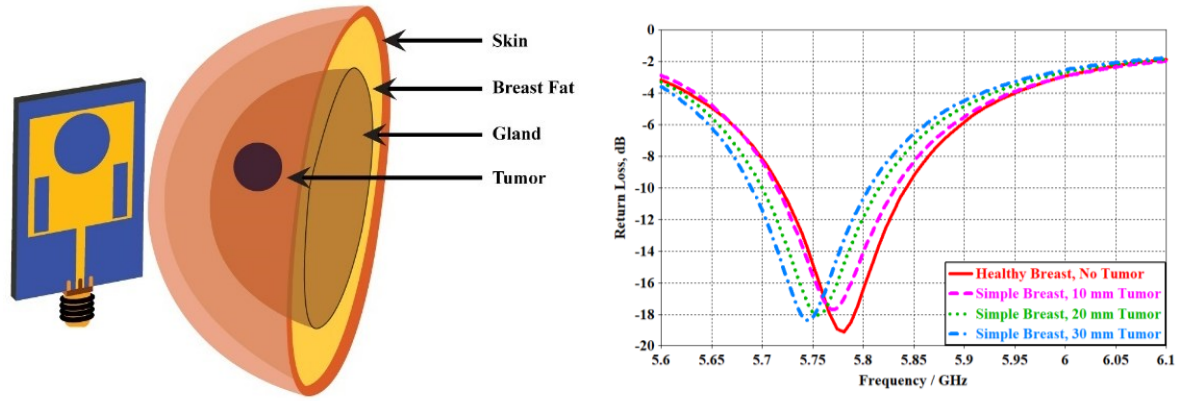

(a) tumor (b) S_{11}

Figure 13. A 3-D view of breast phantom of different radii tumors

4.3. On Head

Computed tomography (CT), positron emission tomography (PET), magnetic resonance imaging (MRI), ultrasound, and x-ray imaging are common medical diagnostic imaging techniques used to detect cancer, stroke, tumors, and other malignant elements in the human head. Negative aspects of computed tomography (CT) and X-ray imaging include exposure to harmful radiation, a high rate of false negatives, decreased susceptibility, and an increased risk of cancer due to both the duration and intensity of exposure [46], [47]. While the MRI method aids doctors in investigating the human body for the presence of specific disorders, it is more costly and less effective than alternative methods. Additionally, ultrasound is superior for some disorders but cannot provide an accurate picture. Although PET scanning technology can differentiate between malignant and noncancerous cells (i.e., tumors), its main drawback is that it may create severe complications for pregnant women [48]. Numerous studies have been conducted in recent years to develop imaging systems of the human body utilizing microwave technology for the early detection and diagnosis of a wide range of disorders, such as cancer, tumors, strokes, and internal bleeding in the brain [39-41]. There are six types of tissue in a human head: skin, fat, muscle, bone, or skull, CSF (cerebrospinal spinal fluid), and dura. The

https://doi.org/10.31436/iiumej.v26i1.3221

suggested antenna was designed and run through the CST simulator. The phantom human head was placed next to the antenna, modeled in free space, and illustrated in Figure 14.

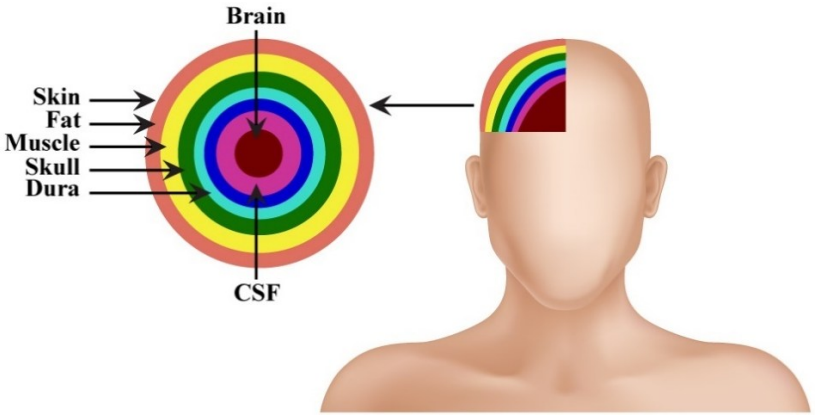

Figure 14. A 3-D view of the human head phantom

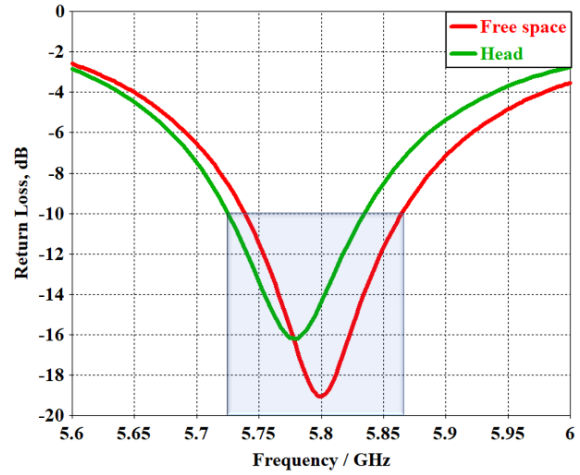

(a) S_{11}

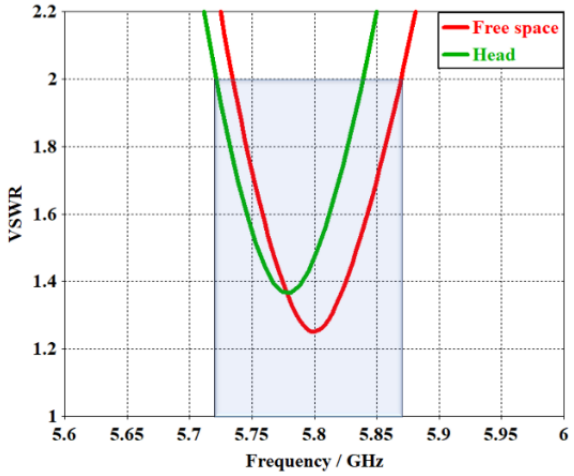

(b) VSWR

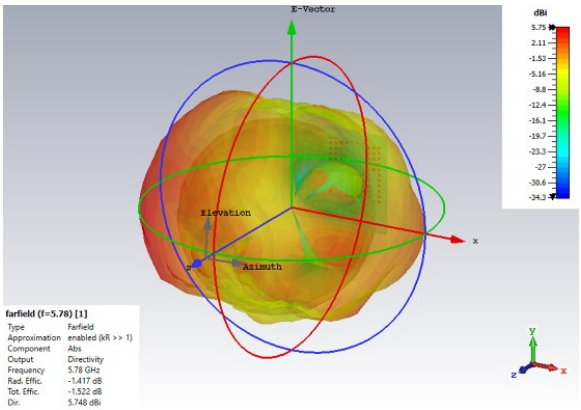

(c) 3D Radiation Pattern at 5.78 GHz

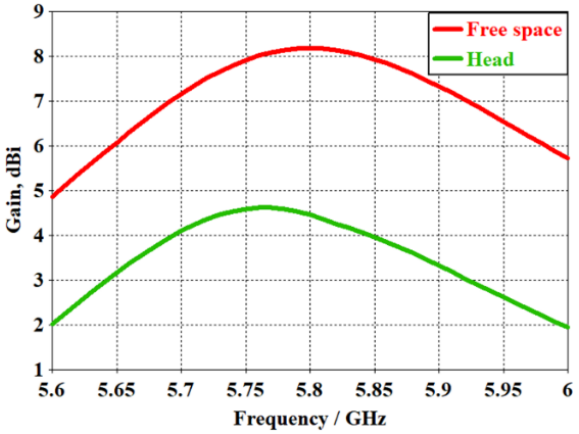

(d) Gain

Figure 15. The simulated results of the human head phantom

A simulation performed on a human head phantom revealed respectable values of the reflection coefficient and VSWR with satisfactory impedance matching from the antenna at 5.78 GHz, as shown in Figure 15(a)(b). The DSSRS antenna has achieved (5.725–5.834) GHz bandwidth of resonant frequency 5.78 GHz on the human head phantom. Figure 15(c)(d)

https://doi.org/10.31436/iiumej.v26i1.3221

illustrates the 3-D radiation pattern and gain. It has been observed that the 3-D radiation pattern is directed toward the Z-axis; on the other hand, the 4.59 dBi gain was achieved at 5.78 GHz on the human head phantom. The SAR can gauge an antenna's suitability for biomedical applications. It was found that from Figure 16, the suggested antenna had a maximum average SAR of 0.0635 W/kg for 1 gm of tissue and 0.0344 W/kg for 10 gm of tissue. There will be no harmful effects from having the values so close to the head. The identification of head tumors is the primary objective of the proposed antenna.

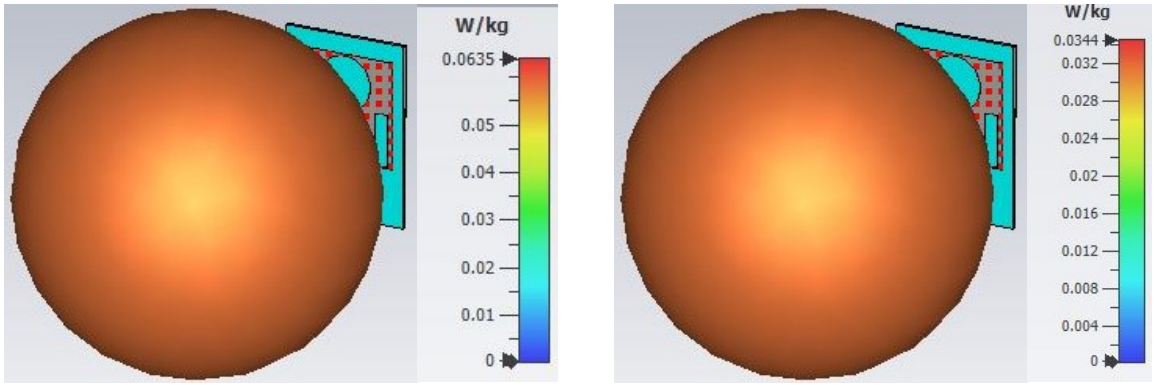

(a) 1 gm (0.0635 W/Kg) (b) 10 gm (0.0344 W/Kg)

Figure 16. The SAR evaluation at 5.78 GHz

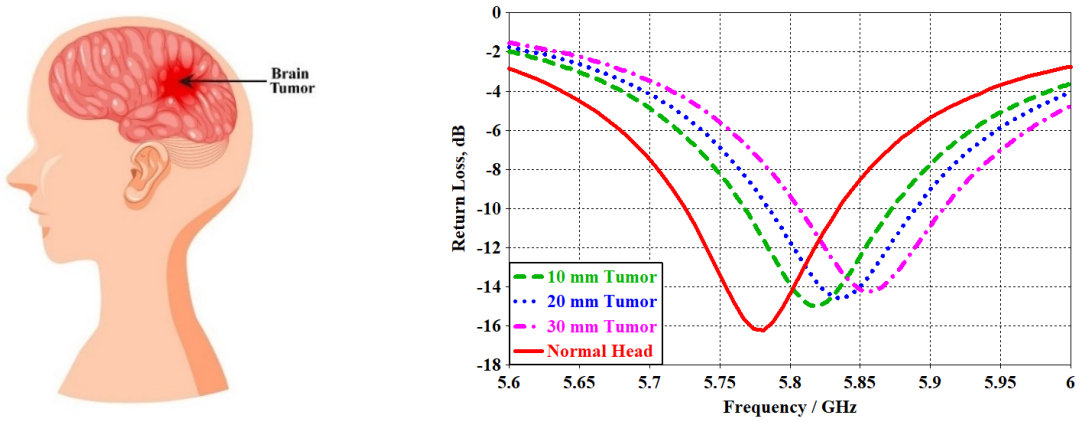

(a) tumor (b) S_{11}

Figure 17. A 3-D view of the head phantom of different radii tumors

The characteristics of fictitious tumors in the head are shown in Figure 17(a) (ε_r=68, σ =0.13[S/m], δ=5.46[W/(m*K)]). Figure 17(b) shows the simulated S_{11} with attenuation of f_r=5.82GHz, –14.973 dB; f_r=5.84GHz, –14.572 dB, and f_r=5.86 GHz, –14.237 dB for tumors with 10, 20, and 30 mm radii, respectively. These simulations aim to test the antenna's performance while a head phantom has a tumor. The value of return loss is slightly higher than it would be in the case of normal tissues, and the resonance frequencies are shifted towards the right as the sizes of the tumor increase, as shown in Figure 17(b). This is demonstrated by the fact that it exhibits the presence of tumors. The distinct characteristics of breast and head tumors result in changes in resonant frequencies, decreases in breast tumors, and increases in head tumors, respectively. This different behavior may be caused by the dielectric and thermal properties of tumors in the breast and head being different in nature. Hence, for accurate detection of the tumors in different body parts, their dielectric and thermal properties and impacts on resonance frequencies must be known earlier. Table 1 summarizes the results achieved with previously developed jeans substrate antenna designs, respectively.

https://doi.org/10.31436/iiumej.v26i1.3221

Table 1. In-depth analysis of the proposed DSSRS antenna versus existing antenna models with the operating frequency in ISM band (GHz)

Ref.	Antenna Design	Substrate	h (mm)	ε_r	Max. Gain (dBi)	SAR (W/kg)					
						Body		Breast		Head	
						1gm	10gm	1gm	10gm	1gm	10gm
[27]	Coplanar keyhole antenna	Nylon blend	---	1.50	2.76	---	---	---	---	---	---
[28]	AMC structure	Polyester textile	4.58	2.20	8.92	0.00103	0.000349	---	---	---	---
[29]	8-shaped EBG structure	Denim	0.8	1.70	---	0.6	0.056	---	---	---	---
[30]	Single patch MIMO antenna	Taffeta fabric	0.98	1.30	---	---	---	---	---	---	---
[32]	RPA	Jeans fabric	1.34	1.78	---	---	---	---	---	---	0.9555
[33]	AMC embedded antenna	Leather	2	2.75	7.47	3.0	---	---	---	6.28	---
[34]	Mercedes Benz logo	Rogers 4003C	0.508	3.38	7.3	0.17	0.09	---	---	---	---
[35]	Comb-shape patch antenna	Denim textile	---	1.7	4.67	1.4	---	---	---	---	---
[36]	Slotted circular patch antenna	ROGER 3010	1.6	10.2	---	1.8	0.3	---	---	---	---
[37]	Pentagon patch antenna	RT/Duroid 5880	1.524	2.2	6.71	---	---	---	---	0.69	0.26
This work	**DSSRS antenna**	**Jeans textile**	**1**	**1.7**	**8.18**	**0.00000662**	**0.0000027**	**0.651**	**0.419**	**0.0635**	**0.0344**

Table 2. Comparison with recent jeans substrate antenna

Ref.	Type of Material	Simulated S_{11} (GHz)	Measured S_{11} (GHz)	Simulated Gain (dBi)	Measured Gain (dBi)	SAR (W/kg)	
						1 gm	10 gm
[41]	Jeans	0.9–6, –25	0.85–6.5, –23.50	2.44	---	---	---
[49]	Jeans	2.2–2.53, –37	2.1–2.54, –36	---	---	---	---
[50]	Jeans	2.42–2.484, 5.5–6.3, –12.80	1.72–2.9, 5.73–5.85, –12.50	---	---	---	---
[51]	Denim	2.4–2.48, –40	2.42–2.47, –33	7.1	---	---	---
[52]	Jeans	2.42–2.49, –34	2.44–2.51, –23.30	7.47	---	Chest:0.0257; Arm:0.0358	---
[53]	Jeans	2.96–12, –50	2.96–11, –23	6.2	5.47	---	Body: 1.6018
This work	**Jeans**	**5.79–5.87, –19.07**	**---**	**8.18**	**---**	**Breast: 0.651; Head: 0.0635**	**Breast:0.419; Head: 0.0344**

5. CONCLUSION

This work presents an illustration of the design of the DSSRS wearable textile monopole antenna for BAN and tumors (breast & head) detection. The structure of the DSSRS antenna, which enables it to operate at the ISM band, makes it appropriate for tumor detection. Tumor detection in areas such as the breast and head operates on the same principle, where the backscatter from the S_{11} parameter provides data for microwave imaging. This study utilized the same antenna for observing tumors in both the breast and head, demonstrating that the

proposed antenna performs very well in both applications, irrespective of gain variation. The proposed antenna is compact in size and has good impedance matching, radiation pattern, and gain while maintaining lower SAR values, making it suitable for use in applications involving wearable devices and breast and brain tumors. In addition, the antenna is tested (by simulation) in various bending scenarios. The antenna has almost the same agreement as the flat surface antenna in bending mode. Findings suggest that the developed compact textile antenna operating in the ISM band is a promising candidate for wearable applications. To validate this work, we conducted a benchmarking study comparing our results with similar studies in the literature. Tables 1 and 2 summarize comparisons based on material, gain, frequency band, and SAR values. Most studies provided simulated SAR readings, while measurements focused on VSWR, S_{11}, and gain. The results presented in this manuscript through simulation are consistent with those in the tables.

ACKNOWLEDGMENT

The authors are very thankful to the International Islamic University Malaysia (IIUM) for the research group program under grant FRGS/1/2024/TK08/UIAM/02/1.

REFERENCES

[1] M. M. H. Mahfuz *et al.*, "Wearable Textile Patch Antenna: Challenges and Future Directions," *IEEE Access*, vol. 10, pp. 38406–38427, 2022.

[2] S. Noor, N. Ramli, and N. Liyana Hanapi, "A Review of the Wearable Textile-Based Antenna using Different Textile Materials for Wireless Applications," *Open J. Sci. Technol.*, vol. 3, no. 3, Art. no. 3, Oct. 2020.

[3] K. N. Paracha, S. K. Abdul Rahim, P. J. Soh, and M. Khalily, "Wearable Antennas: A Review of Materials, Structures, and Innovative Features for Autonomous Communication and Sensing," *IEEE Access*, vol. 7, pp. 56694–56712, 2019.

[4] S. G. Kirtania *et al.*, "Flexible Antennas: A Review," *Micromachines*, vol. 11, no. 9, Art. no. 9, Sep. 2020.

[5] M. U. Ali Khan, R. Raad, F. Tubbal, P. I. Theoharis, S. Liu, and J. Foroughi, "Bending Analysis of Polymer-Based Flexible Antennas for Wearable, General IoT Applications: A Review," *Polymers*, vol. 13, no. 3, Art. no. 3, Jan. 2021.

[6] D. N. Elsheakh, R. A. Mohamed, O. M. Fahmy, K. Ezzat, and A. R. Eldamak, "Complete Breast Cancer Detection and Monitoring System by Using Microwave Textile Based Antenna Sensors," *Biosensors*, vol. 13, no. 1, p. 87, 2023.

[7] A. R. Chishti *et al.*, "Optically Transparent Antennas: A Review of the State-of-the-Art, Innovative Solutions and Future Trends," *Appl. Sci.*, vol. 13, no. 1, Art. no. 1, Jan. 2023.

[8] K. Ghaffarzadeh and J. Hayward, "Stretchable and Conformable Electronics: Heading Toward Market Reality," *Inf. Disp.*, vol. 33, no. 6, pp. 28–31, Nov. 2017.

[9] K. S, N. R, and K. Venusamy, "Recent Trends in Microstrip Patch Antenna Using Textile Applications," Computer-Assisted Learning for Engaging Varying Aptitudes: From Theory to Practice. Accessed: Jan. 13, 2023.

[10] T. Nahar and S. Rawat, "A Survey on Wearable Antenna Used for Defense Applications," in *Flexible Electronics for Electric Vehicles*, S. Dwivedi, S. Singh, M. Tiwari, and A. Shrivastava, Eds., in Lecture Notes in Electrical Engineering. Singapore: Springer Nature, 2023, pp. 121–130.

[11] N. Vikram, R. S. Sabeenian, M. Nandhini, and V. Visweeshwaran, "Design and Implementation of Microstrip Patch Antenna for Biomedical Application," in *International Conference on Innovative Computing and Communications*, D. Gupta, A. Khanna, S. Bhattacharyya, A. E.

Hassanien, S. Anand, and A. Jaiswal, Eds., in Lecture Notes in Networks and Systems. Singapore: Springer Nature, 2023, pp. 613–620.

[12] S. Merugu, A. Kumar, and G. Ghinea, "Real-Time Health Monitoring Using Wearable Devices," in *Track and Trace Management System for Dementia and Intellectual Disabilities*, S. Merugu, A. Kumar, and G. Ghinea, Eds., in Advanced Technologies and Societal Change. , Singapore: Springer Nature, 2023, pp. 119–122.

[13] F. Amitrano, A. Coccia, L. Donisi, G. Pagano, G. Cesarelli, and G. D'Addio, "Gait Analysis using Wearable E-Textile Sock: an Experimental Study of Test-Retest Reliability," in *2021 IEEE International Symposium on Medical Measurements and Applications (MeMeA)*, Jun. 2021, pp. 1–6.

[14] M. M. Mahfuz, M. Islam, M. Habaebi, and J. Chebil, "Design of Wearable Textile Patch Antenna Using C-Shape Etching Slot," *Int. J. Interact. Mob. Technol. IJIM*, p. 2022, Apr. 2022.

[15] K. Guido and A. Kiourti, "Wireless Wearables and Implants: A Dosimetry Review," *Bioelectromagnetics*, vol. 41, no. 1, pp. 3–20, Jan. 2020.

[16] "ICNIRP." Accessed: Jan. 25, 2024. [Online]. Available: https://www.icnirp.org/en/differences.html

[17] A. M. Tripathi, P. K. Rao, and R. Mishra, "An AMC Inspired Wearable UWB Antenna for Skin Cancer Detection," in *2020 International Conference on Electrical and Electronics Engineering (ICE3)*, Feb. 2020, pp. 475–480.

[18] G. K. Soni, D. Yadav, and A. Kumar, "Design consideration and recent developments in flexible, transparent and wearable antenna technology: A review," *Trans. Emerg. Telecommun. Technol.*, vol. 35, no. 1, p. e4894, 2024.

[19] T. A. Karthikeyan, M. Nesasudha, S. Saranya, and B. Sharmila, "A review on fabrication and simulation methods of flexible wearable antenna for industrial tumor detection systems," *J. Ind. Inf. Integr.*, vol. 41, p. 100673, Sep. 2024.

[20] T. Saeidi *et al.*, "Miniaturized Spiral UWB Transparent Wearable Flexible Antenna for Breast Cancer Detection," in *2020 International Symposium on Networks, Computers and Communications (ISNCC)*, Oct. 2020, pp. 1–6.

[21] N. Narang, "Compact Wideband Microstrip Patch Antenna Design for Breast Cancer Detection," *Def. Sci. J.*, vol. 71, p. 352, May 2021.

[22] S. Bhavani and T. Shanmuganantham, "Wearable Antenna for Bio Medical Applications," in *2022 IEEE Delhi Section Conference (DELCON)*, Feb. 2022, pp. 1–5.

[23] N. Jebali, "Textile Ultra-Wide Band Antenna With X Band For Breast Cancer Detection," *Indian J. Sci. Technol.*, vol. 13, no. 11, pp. 1232–1242, Mar. 2020.

[24] Y. Rahayu and R. Saputra, "Design Strategy on Medical Wearable Antenna for Tumor Detection," in *2020 International Symposium on Antennas and Propagation (ISAP)*, Jan. 2021, pp. 105–106.

[25] S. Sinha, T.-S. R. Niloy, R. R. Hasan, Md. A. Rahman, and S. Rahman, "A Wearable Microstrip Patch Antenna for Detecting Brain Tumor," in *2020 International Conference on Computation, Automation and Knowledge Management (ICCAKM)*, Jan. 2020, pp. 85–89.

[26] A. T. Baklezos, C. D. Nikolopoulos, and C. N. Capsalis, "A Planar On-Body Antenna System for Cancerous Tumor Detection through Microwave Transmission Sensing," *J. Electr. Eng.*.

[27] U. Hasni, M. E. Piper, J. Lundquist, and E. Topsakal, "Screen-Printed Fabric Antennas for Wearable Applications," *IEEE Open J. Antennas Propag.*, vol. 2, pp. 591–598, 2021.

[28] W. Bouamra, I. Sfar, A. Mersani, L. Osman, and J. M. Ribero, "A Low-Profile Wearable Textile Antenna Using AMC for WBAN Applications at 5.8GHz," *Eng. Technol. Appl. Sci. Res.*, vol. 12, no. 4, pp. 9048–9055, Aug. 2022.

[29] V. R. Keshwani, P. P. Bhavarthe, and S. S. Rathod, "Eight shape electromagnetic band gap structure for bandwidth improvement of wearable antenna," *Prog. Electromagn. Res. C*, vol. 116, pp. 37–49, 2021.

[30] C. Loss, T. M. Silveira, P. Pinho, R. Salvado, and N. B. de Carvalho, "Design and Analysis of the Reproducibility of Wearable Textile Antennas," in *2020 12th International Symposium on Communication Systems, Networks and Digital Signal Processing (CSNDSP)*, Jul. 2020, pp. 1–5.

[31] P. Balaji and R. Narmadha, "Wearable E-shaped Textile Antenna for Biomedical Telemetry," in *2021 International Conference on Advances in Electrical, Computing, Communication and Sustainable Technologies (ICAECT)*, Feb. 2021, pp. 1–5.

[32] R. S. Campos and F. D. R. Henriques, "Performance evaluation of a microstrip wearable antenna considering on-body curvature," *Int. J. Eng. Sci.*, vol. 11, no. 10, pp. 8–19, 2021.

[33] P. Saha, D. Mitra, and S. K. Parui, "Control of Gain and SAR for Wearable Antenna Using AMC Structure," *Radioengineering*, vol. 30, no. 1, pp. 81–88, Apr. 2021.

[34] S. Kiani, P. Rezaei, and M. Fakhr, "A CPW-fed wearable antenna at ISM band for biomedical and WBAN applications," *Wirel. Netw.*, vol. 27, no. 1, pp. 735–745, Jan. 2021.

[35] D. Gopi, P. V. Kokilagadda, S. Gupta, and V. R. K. R. Dodda, "Asymmetric coplanar strip-fed textile-based wearable antenna for MBAN and ISM band applications," *Int. J. Numer. Model. Electron. Netw. Devices Fields*, vol. n/a, no. n/a, p. e2920.

[36] G. Narmadha, M. Malathi, S. A. Kumar, T. Shanmuganantham, and S. Deivasigamani, "Performance of implantable antenna at ISM band characteristics for biomedical base," *ICT Express*, vol. 8, no. 2, pp. 198–201, Jun. 2022.

[37] S. Alhuwaidi and T. Rashid, "A Novel Compact Wearable Microstrip Patch Antenna for Medical Applications," in *2020 International Conference on Communications, Signal Processing, and their Applications (ICCSPA)*, Mar. 2021, pp. 1–6.

[38] G. S. Deepthy and M. Nesasudha, "Analysis of substrate materials in microstrip antenna for biomedical applications," *Mater. Today Proc.*, Jan. 2023.

[39] C. A. Balanis, *Antenna Theory: Analysis and Design*. John Wiley & Sons, 2016.

[40] D. M. G. Preethichandra, L. Piyathilaka, U. Izhar, R. Samarasinghe, and L. C. De Silva, "Wireless Body Area Networks and Their Applications – A Review," *IEEE Access*, pp. 1–1, 2023.

[41] F. Khajeh-Khalili and Y. Khosravi, "A novel wearable wideband antenna for application in wireless medical communication systems with jeans substrate," *J. Text. Inst.*, vol. 112, no. 8, pp. 1266–1272, Aug. 2021.

[42] M. Faisal, A. Gafur, S. Z. Rashid, Md. O. Shawon, K. I. Hasan, and Md. B. Billah, "Return Loss and Gain Improvement for 5G Wireless Communication Based on Single Band Microstrip Square Patch Antenna," in *2019 1st International Conference on Advances in Science, Engineering and Robotics Technology (ICASERT)*, Dhaka, Bangladesh: IEEE, May 2019, pp. 1–5.

[43] V. Karthik and T. Rama Rao, "Investigations on SAR and Thermal Effects of a Body Wearable Microstrip Antenna," *Wirel. Pers. Commun.*, vol. 96, no. 3, pp. 3385–3401, Oct. 2017.

[44] N. Sharma, A. Kumar, A. De, and R. K. Jain, "Design of compact hexagonal shaped multiband antenna for wearable and tumor detection applications," *Prog. Electromagn. Res. M*, vol. 105, pp. 205–217, 2021.

[45] J. E. Lara, A. Vera, and L. Leija, "Proposal for the application of microwave ablation as a treatment for breast cancer using interstitial applicators: Antenna design and FEM modeling," in *2016 Global Medical Engineering Physics Exchanges/Pan American Health Care Exchanges (GMEPE/PAHCE)*, Apr. 2016, pp. 1–6.

[46] K. Kerlikowske, C. C. Gard, B. L. Sprague, J. A. Tice, and D. L. Miglioretti, "One versus Two Breast Density Measures to Predict 5- and 10-Year Breast Cancer Risk," *Cancer Epidemiol. Biomarkers Prev.*, vol. 24, no. 6, pp. 889–897, Jun. 2015.

[47] H. Been Lim, N. Thi Tuyet Nhung, E.-P. Li, and N. Duc Thang, "Confocal Microwave Imaging for Breast Cancer Detection: Delay-Multiply-and-Sum Image Reconstruction Algorithm," *IEEE Trans. Biomed. Eng.*, vol. 55, no. 6, pp. 1697–1704, Jun. 2008.

[48] A. Alikhassi *et al.*, "False-positive incidental lesions detected on contrast-enhanced breast MRI: clinical and imaging features," *Breast Cancer Res. Treat.*, Feb. 2023.

[49] A. Ashyap *et al.*, "Inverted E-Shaped Wearable Textile Antenna for Medical Applications," *IEEE Access*, vol. PP, pp. 1–1, Jun. 2018.

[50] K. Wang and J. Li, "Jeans Textile Antenna for Smart Wearable Antenna," in *2018 12th International Symposium on Antennas, Propagation and EM Theory (ISAPE)*, Dec. 2018, pp. 1–3.

[51] P. M. Potey and K. Tuckley, "Design of wearable textile antenna for low back radiation," *J. Electromagn. Waves Appl.*, vol. 34, no. 2, pp. 235–245, Jan. 2020.

[52] A. Y. I. Ashyap *et al.*, "Fully Fabric High Impedance Surface-Enabled Antenna for Wearable Medical Applications," *IEEE Access*, vol. 9, pp. 6948–6960, 2021.

[53] A. Yadav, V. Kumar Singh, A. Kumar Bhoi, G. Marques, B. Garcia-Zapirain, and I. de la Torre Díez, "Wireless Body Area Networks: UWB Wearable Textile Antenna for Telemedicine and Mobile Health Systems," *Micromachines*, vol. 11, no. 6, Art. no. 6, Jun. 2020.